Original Articles

Assessing drivers of intra-seasonal grassland dynamics in a Kenyan savannah using digital repeat photography

James M. Muthoka [a,*], Alexander S. Antonarakis [a], Anton Vrieling [b], Francesco Fava [c], Edward E. Salakpi [d], Pedram Rowhani [a]

[a] *Department of Geography, University of Sussex, Brighton BN1 9QJ, UK*
[b] *University of Twente, Faculty of Geo-information Science and Earth Observation, 7500 AE Enschede, Netherlands*
[c] *Department of Environmental Science and Policy, Università degli Studi di Milano, Via Celoria 2, 20133 Milano, Italy*
[d] *Department of Physics and Astronomy, University of Sussex, Brighton BN1 9QH, UK*

ARTICLE INFO

ABSTRACT

Understanding grassland dynamics and their relationship to weather and grazing is critical for pastoralists whose livelihoods depend on grassland productivity. Studies investigating the impacts of climate and human factors on inter-seasonal grassland dynamics have focused mostly on changes to vegetation structure. Yet, quantifying the impact of these on the inter-seasonal dynamics of specific grassland communities is not known. This study uses digital repeat photography to examine how intra-seasonal grassland dynamics of different grassland communities are affected by precipitation, temperature, and grazing in a heterogeneous semi-arid savannah in Kenya. A low-cost digital repeat camera network allowed for fine-scale temporal and spatial variability analysis of grassland dynamics and grazing intensity. Over all grass communities, our results show precipitation driving mainly early-season and in some cases mid-season flushing, temperature driving end-of-season senescence, and grazing influencing mid-season declines. Yet, our study quantifies how these three drivers do not uniformly impact grassland species communities. Specifically, *Cynodon* and *Cynodon/Bothriochloa* communities are rapidly and positively associated with precipitation, where mid-season declines in Cynodon communities are associated with grazing and late-season declines in *Cynodon/Bothriochloa* communities are associated with temperature increases. Setaria communities, on the other hand, have weaker associations with the drivers, with limited positive associations with precipitation and grazing. *Kunthii/Digitaria* diverse communities had no association with the three drivers. Highly diverse mixed communities were associated with increased precipitation and temperature, as well as lower intensity grazing. Our research sheds light on the complex interactions between plants, animals, and weather. Furthermore, this study also demonstrates the potential of digital repeated photography to inform about fine-scale spatial and temporal patterns of semi-arid grassland vegetation and grazing, with the goal of assisting in the formulations of management practises that better capture the intra-annual variability of highly heterogeneous dryland systems.

1. Introduction

Grasslands cover more than one-third of the global land area (Reynolds et al., 2005). They are critical for food security (Boval & Dixon, 2012; O'Mara, 2012), ecological services (Bengtsson et al., 2019), carbon sequestration (Yang et al., 2019), and cultural heritage (Mire, 2017). In African drylands, grasslands are also vital to pastoralist communities who rely on them as the primary source of fodder for their livestock (Reid et al., 2008). Their livelihoods depend on regular access

to palatable pastures, but pastoralists also significantly contribute to local, national, and regional economies (Caroline King-Okumu et al., 2015; Republic of Kenya, 2012, 2021). Changes to grassland productivity, particularly when they happen within the season, can therefore substantially impact food security, and cause wider socio-economic and ecological implications. Yet little is known about these intra-seasonal grassland dynamics and the corresponding drivers in the drylands.

In Kenya, grasslands support pastoralism, a sector worth US$1.13 billion in the country's economy (Nyariki & Amwata, 2019). Further,

---

they are the primary food source for the livestock and pastoralist communities (Mganga et al., 2015) and represent rich plant biodiversity (Akwee et al., 2017; Cheche et al., 2015; Jawuoro et al., 2017). However, grasslands are under threat of degradation due to the shifting land management practices (Said et al., 2016), overgrazing (Kioko et al., 2012), invasive plant species (Githae, 2018; Muthoka et al., 2021; Strum et al., 2015), and a changing climate (Nicholson, 2014).

Several studies have described the effects of climate and human intervention on grassland dynamics across different regions and seasons (Linderman et al., 2010; Liu et al., 2019a, 2021; Zarei et al., 2021). Mostly, these studies focused on disentangling the role of climate and human factors in grassland inter-seasonal dynamics and long-term degradation trends (Liu, Wang, et al., 2019; Polley et al., 2014; Yu et al., 2022) but less on distinguishing the specific roles of weather variation and human activities such as grazing on seasonal grassland dynamics. The few studies that looked at seasonal vegetation dynamics mostly differentiated the dynamics based on the vegetation structure (D'Adamo et al., 2021; Liu et al., 2021; Tong et al., 2019) but not on species composition, although weather and grazing impacts may differ depending on plant community composition and diversity (Ondier et al., 2019). Also, previous research has not looked into separately quantifying the effect of grassland communities, weather and grazing factors. As a result, the impacts of species composition, precipitation, temperature, and grazing on semi-arid savannah grassland seasonal dynamics are still unclear (Cheng et al., 2020).

Earth Observation, specifically satellite remote sensing and *in-situ* digital cameras (phenocams), is a valuable tool for studying the impacts of climate and grazing on grassland dynamics (D'Adamo et al., 2021; Gómez-Giráldez et al., 2020; Zhou et al., 2017). Due to its spatial and temporal coverage, satellite imagery allows assessing grassland productivity and phenology for larger regions (Caparros-Santiago et al., 2021; Reinermann et al., 2020). However, cloud cover, high data dimensionality and costs, especially for high-resolution data, are drawbacks of using satellite remote sensing (Ali et al., 2016). As an alternative, phenocams are a low-cost, "near ground" tool for collecting frequent and spatially-detailed information on vegetation dynamics (Richardson, 2019). In addition, it offers an automated observation of vegetation dynamics instead of direct visual observations by dedicated field staff volunteers (van Vliet et al., 2014). Phenocams are stationary digital cameras set up in the field to take repeated pictures at predetermined intervals, allowing for the temporal tracking of phenology. Vegetation indices derived from phenocams can effectively measure fine-scale changes in greenness (Cheng et al., 2020; Matongera et al., 2021). Therefore, the deployment of inexpensive digital repeat cameras across different grassland communities can provide an effective approach to understanding how their productivity and dynamics vary throughout the season as a function of species composition, weather, and grazing. However, despite the use of digital repeat cameras in a variety of biomes, ecosystems, and regions with much focus on the United States, China, Japan, the United Kingdom, and Malaysia, digital repeat cameras have not been used frequently in Africa's semi-arid savannah grasslands (Cheng et al., 2020; Jonge et al., 2022; Seyednasrollah et al., 2019; D. Yan et al., 2019).

This paper aims to understand how grassland communities, precipitation, temperature, and grazing affect grassland dynamics in a semi-arid grassland located in Kenya's Kapiti research station. A time series of digital repeat photographs acquired by a network of seven digital cameras in 2019 is used to determine changes in the grassland community's greenness and estimate the number of wild and domestic grazers. In addition, the dataset was used to evaluate relationships with key drivers of grassland dynamics selected based on the existing literature (Ondier et al., 2019; Polley et al., 2014; Yan et al., 2019; Yu et al., 2012; Zarei et al., 2021; Zhang et al., 2018). A better understanding of the fine-scale spatial variations and the rapid temporal dynamics is essential for providing insights into the complexity of rangelands in arid and semi-arid environments.

2. Study area and data

2.1. Study area

The research was conducted at the Kapiti research station (Fig. 1), located in Machakos County at an altitude of 1615–1920 m above sea level (m.a.s.l). The International Livestock Research Institute (ILRI) owns the station, covering 128 km^2. It is home to approximately 2500 cattle herds and 1450 sheep and goats (ILRI, 2019). Furthermore, it serves as an important migration corridor for wild animals migrating from Nairobi National Park to Tsavo National Park. However, as urban infrastructure development has increased across and around the migration corridor, the research station has become a haven for wildlife, including herbivores and carnivores.

The Kapiti research station is located in a semi-arid land. It receives annual average precipitation of 550 mm (ILRI, 2019) over two seasons (i.e. "long rains" in March, April, and May and "short rains" in October, November, and December). Herbaceous plants (i.e., grasses and forbs) and patchy savanna woody species such as *Acacia nubica* dominate the farm's vegetation. Additionally, the herbaceous species include perennials (e.g., *Setaria trinervia, Themeda triandra, Cynodon dactylon, Digitaria macroblephara, Microchloa kunthii*), annuals (e.g., *Eragrostis tenuifolia, Aristida keniensis, Lolium temulantum*), and forbs (e.g., *Blepharis hildebrandtii, Sida ovata, Schkuhria*). The research station's major soils are red cotton in the ridges and black cotton in the plains, with patches of sandy soils primarily along ephemeral channels (ILRI, 2019).

2.2. Data

2.2.1. Grassland community surveys and soil properties

During a field campaign undertaken between April and July 2019, two 3 km-long transects running East-West (EW) and North-South (NS) were identified (see Fig. 1) for detailed site sampling of herbaceous composition and soil properties across different vegetation communities, grazing characteristics, and slope gradients (Table 1). In the two transects, initially, we had more grassland sites sampled; however, due to camera malfunction, not all were retained for the analysis. Both livestock and wildlife graze these areas, and the elevation is relatively uniform, ranging from 1631 to 1685 m.a.s.l. The distance between each sampled site was about 1 km, and each site measured 30 m × 30 m (900 m^2). As a result, the seven grassland sites were chosen in consultation with the Kapiti research station to represent best the community of grasslands and forbs found in the region, including palatable and preferential grasses for livestock and wildlife.

The herbaceous composition was estimated at each grassland site, where four 0.5 m × 0.5 m quadrants were randomly nested in each 900 m^2 sample plot. Next, individual plants of a specific herbaceous species were counted within each quadrant to estimate frequency density and cover, calculated based on the proportion of area covered by the grass compared to the total soil area within the quadrants. Finally, we calculated the cover-abundance values for each plant taxon using the Braun-Blanquet method (Braun-Blanquet, 1932) and saved them in the TURBOVEG program (Hennekens & Schaminée, 2001).

Also, we sampled soil at each site using a cross-diagonal pattern with uniform collection subsamples (i.e., six per diagonal and 12 total for each 900 m^2 sample plot) (Soil Survey Staff, 2014). The subsample was collected at depths of 0–20 cm and 20–40 cm, yielding two composite samples per grassland site. Each composite was thoroughly mixed, and two cups were placed in a sample bag labelled for subsequent laboratory analysis. Finally, soil organic carbon (OC), alkalinity (pH), nitrogen (N), phosphorus (P), and potassium (K) levels were determined for both depths.

2.2.2. Precipitation and temperature data

Precipitation and temperature data were based on an *in-situ* weather station inside the Kapiti research station and situated at a 0.8–3.6 km
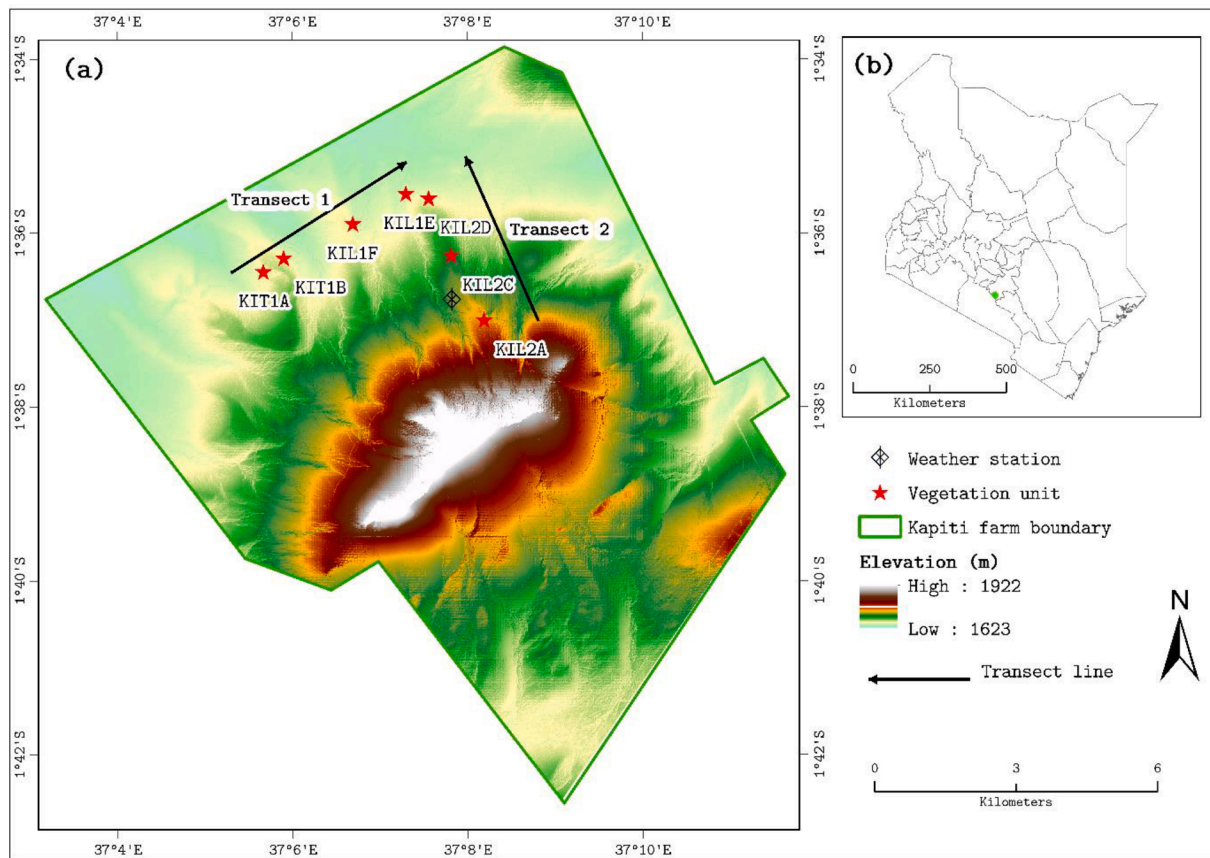
Fig. 1. An overview of the Kapiti research station overlaid on a 5 m resolution Digital Terrain Model of the study area, which was generated from data acquired with a Leica ALS60 aerial LIDAR (panel a) as well as the grassland site locations. Plotted alongside is a map showing the study location in Kenya (panel b).

Table 1
Description of the grassland sites.

Transect	Site	Latitude	Longitude	Elevation (m)	Soils	Site description
1	KIT1A	−1.607	37.094	1638	Clay and loam	Open grasslands with sparse shrub vegetation are dominated by herbaceous cover (90 %). Located about 200 m away from an active sheep and goat "boma" and grazed by both livestock and wildlife.
	KIT1B	−1.604	37.098	1639	Clay	Open grasslands with sparse shrub vegetation are dominated by the herbaceous cover (90 %). Located 500 m away from a watering pan and is grazed by livestock and wildlife.
	KIL1F	−1.598	37.111	1637	Clay and loam	Open grassland with sparse shrub vegetation and dominated by herbaceous cover (90 %). This site is grazed by both wildlife and livestock.
	KIL1E	−1.591	37.121	1631	Clay (deep back cotton)	Mixed grassland and shrubs vegetation dominated by the herbaceous cover (60 %). Located in an area susceptible to flooding with structurally high herbaceous species characterised by low animal grazing.
2	KIL2A	−1.616	37.136	1685	Clay (red cotton)	Open grasslands with sparse shrub vegetation are dominated by the herbaceous cover (90 %). Located in well-drained soils and grazed by both livestock and wildlife. Historically the site was an animal holding unit "boma".
	KIL2C	−1.604	37.130	1659	Clay (red cotton)	Open grassland with sparse shrub vegetation is dominated by the herbaceous cover (90 %). This site is grazed by both wildlife and livestock.
	KIL2D	−1.593	37.126	1636	Clay (deep back cotton)	Mixed grassland and shrubs vegetation dominated by the herbaceous cover (60 % cover). Located in an area susceptible to flooding with structurally high herbaceous species and characterised by low animal grazing.

P – perennial, F - forbs and A – annuals. Dominant species are highlighted in bold.

distance from the seven sampling plots. These data were recorded every 15 min. Temperature measurements were processed to obtain the daily average temperature, whereas precipitation was aggregated to daily precipitation values. In addition, missing data in our precipitation data were filled using CHIRPS (Funk et al., 2015) rainfall estimates from rain gauge and satellite observation; this is after the station broke down.

2.2.3. Near ground digital photography time-series data

Time-series of digital photographs were obtained at each plot with

Bushnell Trophy Cam Essential cameras (i.e., Phenocam) at 12 megapixels and saved in JPEG format. All cameras were programmed to take photos every 30 min for 12 h (0600 – 1800Hrs). All phenocams were installed at approximately 2 m above the ground surface at the southern edge of each plot. They were positioned at an inclination depression angle of at least 8° (Vrieling et al., 2018), ensuring that the camera had a 10–30 m field of view of the plot. We used the data collected from the end of March to the end of July 2019, which corresponds to the long rains growing season.

3. Methods

3.1. Determining grassland community and soil properties

The herbaceous composition data collected during the field campaign were imported into TURBOVEG and then exported into JUICE software (Tichý, 2002) for subsequent statistical analysis. Within JUICE, we statistically computed the herbaceous species richness (R) (i.e. the average number of species in all quadrats in which the species occurs), the herbaceous plant diversity (using the Shannon-Wiener Diversity Index (Equation (1))), the herbaceous species evenness (*E*) (Equation (2)), and the dominant herbaceous species based on cover and frequency threshold of 50 and 60 respectively as outlined by Chytrý et al. (2003). Also, we qualitatively characterized the grassland community based on grassland site herbaceous species composition.

$$H = -\sum_{i=1}^{S} p_i \ln p_i \tag{1}$$

$$E = 1 - \frac{2}{\pi}\arctan\left(\frac{\sum_{i=1}^{S}\left(\ln(p_i) - \frac{\sum_{i=1}^{S}\ln(p_i)}{S}\right)^2}{S}\right) \tag{2}$$

where S is the number of species and p_i is the proportion of the individual species cover relative to the total cover.

The Walkley-Black method described in the FAO (2019) guideline was followed to calculate soil organic carbon (OC) using chromic oxidation. When two volumes of sulfuric acid are mixed with one volume of dichromate acids and one volume of nitrogen potassium, the dichromate solution oxidises oxidisable matter in the soil, generating heat. The remaining dichromate is titrated with ferrous sulphate, the solution of which is inversely proportional to the amount of carbon in the soil. Additionally, the total nitrogen (N), phosphorus (P), and potassium (K) levels in the soil were measured following the guidelines established by Motsara and Roy (2008). First, total N was determined using the modified Kjeldahl method, which employs salicylic acids and converts available organic and inorganic salts into an ammonium form that is distilled and estimated using standard acid at the end of digestion. Second, P was determined using the Olsen method for neutral and alkali soils, which produces coloured compounds when appropriate reagents are added to a solution. The intensity is proportional to the concentration of the elements being estimated. Third, the presence of P in the soil is extracted using one molar neutral ammonium acetate, and finally, the pH was determined using a glass electrode technique (Okalebo et al., 2002).

3.2. Extraction of animal counts from digital photography time-series

This study used animal presence as a proxy for grazing intensity, defined as the daily aggregate of animals found within the phenocam field of view, assuming that presence implies grazing activity. We used the phenocam 30 min time-series photographs to compute an aggregate daily animal presence count by counting individual ruminants (i.e., cattle, sheep, goats, and wildlife) in each picture frame. To detect the animals, we used a pre-trained model called MegaDetector and developed by Microsoft for processing camera trap data (Beery et al., 2019; Microsoft, 2020). MegaDetector model is based on a Faster Region-Based Convolutional Neural Network (RCNN) with an inceptionResNetv2 base network and trained with the TensorFlow Object Detection API with millions of bounding box labels from different habitats. The choice of the model was informed by success in the pre-trained object detection model and application in wildlife ecology (Fennell et al., 2022; Norouzzadeh et al., 2021). MegaDetector model has three categories of classification (i.e., humans, animals, and vehicles) and based on our

interest in deriving grazing intensity, we settled on the animal category. Also, we set critical prediction thresholds of the model at 45 % confidence and did not consider detection with < 45 % confidence. The reader is referred to Beery et al. (2019) for further details on the RCNN algorithm and its implementation. Finally, the model's accuracy in animal detection was evaluated by cross-checking the model counts against visually determined animal counts for seventy randomly selected frames. We computed the root mean square error (RMSE) to assess the difference between the two methods.

3.3. Assessing grassland dynamics from phenocam time-series

We used the "Phenopix" R package (Filippa et al. 2016) to assess changes in vegetation greenness from the photo time series as a proxy of the phenological behaviour of the vegetation within the camera footprint. First, we performed a visual quality check on the image time series and manually removed all blurred photographs or for which an individual animal was directly in front of the camera, prohibiting a good observation of the scene. Then, a Region of Interest (ROI) was created within the phenocam field of view in patches of homogeneous herbaceous species (see Fig. 2). Within the ROIs, we extracted the mean digital numbers (DN) in the red (R), green (G) and blue (B) spectral ranges from each of the photos and derived the Green Chromatic Coordinate (Gcc) (Gillespie et al., 1987), which allowed us to compute the greenness relative to total brightness using Equation (3):

$$\frac{G_{DN}}{R_{DN} + G_{DN} + B_{DN}} \tag{3}$$

where G_{DN}, R_{DN}, and B_{DN} correspond to the digital numbers of green, red, and blue.

While we acknowledge the existence of other indices, such as the green excess index (Woebbecke et al., 1995), we chose to use Gcc due to its extensive use in vegetation and phenology analysis especially employing near ground remote sensing of digital repeat photography (Cheng et al., 2020; Filippa et al., 2016; Richardson, 2019; Seyednasrollah et al., 2019; Vrieling et al., 2018) and its ability to overcome changes in scene brightness (Sonnentag et al., 2012). Additionally, using the extracted ROI-mean, we further filtered the data to reduce noise caused by different illumination by identifying the 90th percentile values based on a three-day moving window as proposed by Sonnentag et al. (2012) and widely used in similar studies (Cheng et al., 2020; Gómez-Giráldez et al., 2020; Seyednasrollah et al., 2019; Vrieling et al., 2018).

3.4. Assessing the drivers of intra-seasonal grassland dynamics

We used quantitative and qualitative analyses to deduce the relationship between changes in vegetation greenness and weather and grazing factors. First, Pearson's correlation coefficient was used to examine the strength and relationship between greenness (Gcc) and precipitation (PRCP), air temperature (AT), and grazing (animal frequency A) factors for the season. Here, we used the number of days that indicated a strong correlation as the minimum number of days that show a change in greenness for the aggregation days. For example, to arrive at the Gcc change, we computed the difference in greenness based on the aggregation periods (4 days representing one lag). Next, we analysed this relationship with multiple lags of PRCP, AT, and A. Previous research has revealed a time lag between vegetation and climatic variables (Pei et al., 2019; Udelhoven et al., 2009; Wen et al., 2019; Wu et al., 2015). Finally, we performed multiple linear regression (Equation (4)) to model the association between Gcc and optimal lags for PRCP, AT, and A at a standard significance level (p = 0.05) with an adjusted R^2 score to compare the same variables across grassland sites, analysed for the relative importance (Gromping, 2006), and making sure we tested for the main linear regression assumptions of normality and
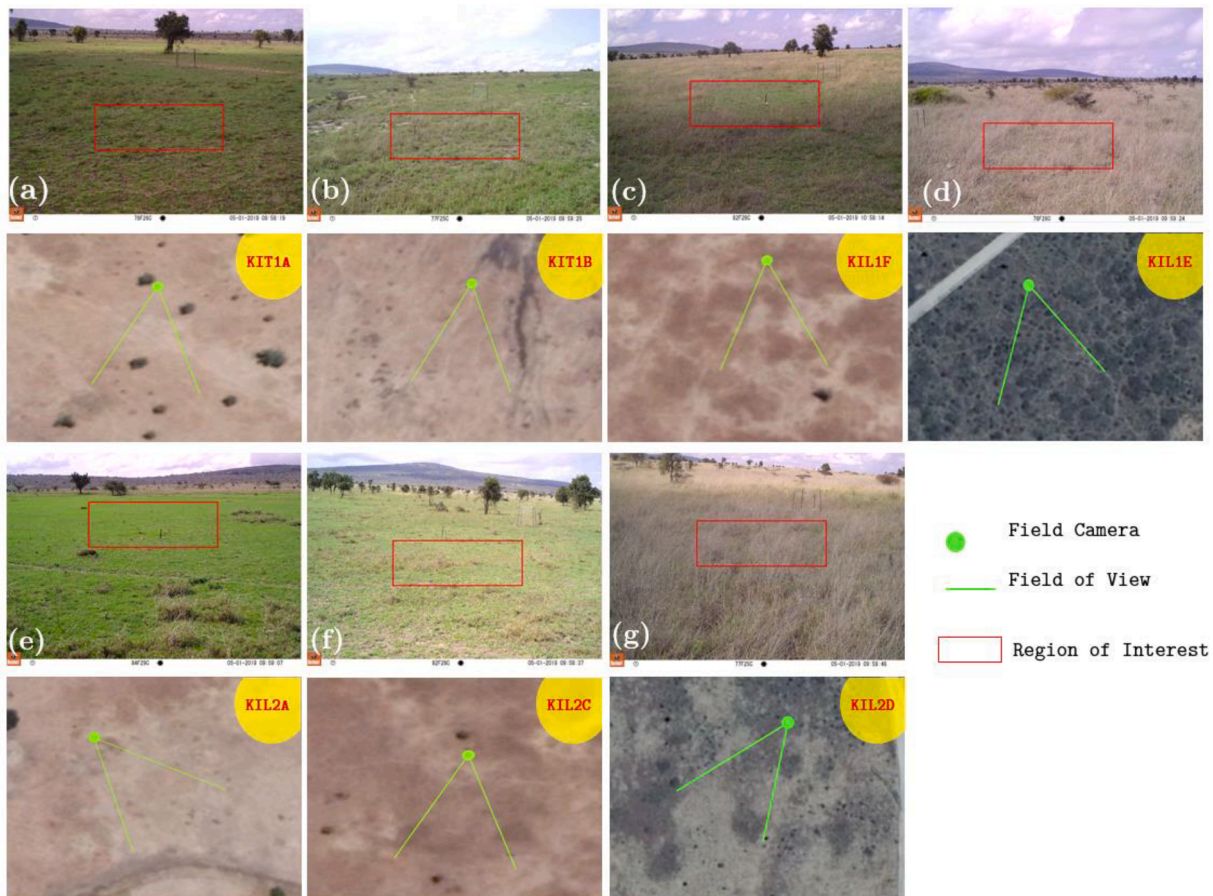
Fig. 2. Panel (a)-(g) shows sample photos taken at Kapiti research station on May 1st, 2019 at 09:59 (EAT) by cameras KIT1A, KIT1B, KIL1F, KIL1E, KIL2A, KIL2C, and KIL2D, respectively. The top row corresponds to the camera position along transect one, while the second row depicts the camera position and field of view draped on the Google Earth image. Panel (e)-(g) correspond to the transect two cameras, as well as camera positions and field of view. The red box depicts the area of interest used to sample and calculate average Gcc values.

multicollinearity (Daoud, 2017; Gareth et al., 2021):

$$y = \beta_0 + \beta_1 X_1 + \beta_2 X_2 + \cdots + \beta_k X_k + \epsilon \qquad (4)$$

where y is the predicted variable (Gcc), β_0 is the y-intercept, β_1, β_2 is the slope, X_1 through X_k is the independent variable (PRCP, AT, A), and β_1 through β_k are the estimated regression coefficients, and ϵ is the model's random error (residual).

4. Results

4.1. Grassland characterization

4.1.1. Analysis of herbaceous composition.

The results on herbaceous species richness, diversity and evenness are presented in Table 2. Overall, 84 herbaceous species were recorded

Table 2
Plant species richness, diversity, and evenness at the various grassland sites.

Grassland site	Species richness (R)	Mean species/ plot	Mean species diversity (H)	Mean species evenness
KIT1A	34	17.50	2.45	0.87
KIT1B	48	22.5	2.48	0.81
KIL1F	39	18.25	2.30	0.80
KIL1E	25	11.00	1.62	0.66
KIL2A	19	8.25	1.36	0.68
KIL2C	42	21.25	2.61	0.86
KIL2D	29	13.00	1.71	0.66

at the Kapiti grasslands, with forbs (54 species) outnumbering grasses (30 species) across all grassland sites. Among the 30 grass species, 22 were perennial, and eight were annual grass species. Also, the heterogeneity among our grassland sites is evident from our analysis presented in the form of species richness, diversity, and evenness. We found single dominant community (KIL1E, KIL2A, and KIL2D) to have the lowest (1.62, 1.36, and 1.71) plant diversity, while co-dominant (KIT1A, KIT1B), and mixed community (KIL1F and KIL2C) to have the highest herbaceous plant diversity (2.45, 2.48, 2.3, and 2.61, respectively). Also, the single dominant community (KIL2A) had a low mean herbaceous species of all grassland communities. Finally, we observed similar species evenness between KIL1E and KIL2D and between co-dominance and mixed community (KIT1A, KIT1B, KIL1F, and KIL2C) grasslands.

Table 3 highlights the results of grassland communities found in the Kapiti grasslands. Our findings show that *Setaria trinervia* (95 %) was the dominant single species at sitesKIL1E and KIL2D (hereafter referred to as "*Setaria* community" and *Cynodon dactylon* (75 %) (hereafter "*Cynodon* community" was the dominant single herbaceous species at site KIL2A. Site KIT1A and KIT1B have co-occurrence of *Bothriochloa insculpta/ Cynodon dactylon* and *Microchloa kunthii/ Digitaria macroblephara*, species o- (hereafter "*Bothriochloa/Cynodon* community and *Kunthii/Digitaria* species"), sites KIL1F and KIL2C. Other species of high frequency included *Mariscus macropus, Sporobolus pyramidalis, Sporobolus discosporus, Euphorbia inaequilatera, Aristida adoensis, Pennisetum mezianum, Craterostigma pumilum, Themeda triandra, Bothriochloa insculpta, Harpachne schimperi, Microchloa kunthii,* and *Indigofera volkensii.*

Table 3

Synoptic table of a semi-arid Kapiti grasslands showing constant species and dominant species.

Grassland community	Species frequency (above 60 %)	Dominant species (above 50 %)
Bothriochloa/ Cynodon (KIT1A)	*Bothriochloa insculpta(P), Craterostigma pumilum(F),* **Cynodon dactylon(P),** *Digitaria macroblephara(P), Eragrostis tenuifolia(P), Indigofera volkensii(F),* **Microchloa kunthii(P),** **Pennisetum mezianum(P),** *Pentanisia ouranogyne(F), Sida ovata(F),* **Sporobolus discosporus(P),** *Themeda triandra(P)*	
Cynodon (KIL2A)	**Cynodon dactylon (P),** *Digitaria scalarum (P),* **Justicia exigua (F),** *Schkuhria pinnata (F)*	75 % - *Cynodon dactylon* (P)
Kunthii/Digitaria (KIT1B)	*Digitaria macroblephara(P), Eragrostis tenuifolia(A), Eustachys paspaloides (P), Hermania alhiensis(F),* **Microchloa kunthii(P),** *Pennisetum mezianum(P), Portulacca kermesina(F), Schkuhria pinnata(F),* **Sida cuneifolia(F),** *Sida ovata(F), Sporobolus pyramidalis(P),* **Themeda triandra(P)**	
Mixed (KIL1F)	*Bothriochloa insculpta(P),* **Craterostigma pumilum(F),** *Crossandra subacaulis(F),* **Digitaria scalarum(P),** **Harpachne schimperi(P),** **Hyparrhenia lintonii(P),** **Indigofera volkensii(F),** **Microchloa kunthii(P),** *Senna mimosoides(F),* **Sida ovata(F),** *Sporobolus pyramidalis(P),* **Themeda triandra(P)**	
Mixed (KIL2C)	**Becium obovatum(F), Bothriochloa insculpta(P),** *Craterostigma pumilum(F),* **Digitaria macroblephara(P),** *Digitaria scalarum(P),* **Harpachne schimperi(P),** **Heteropogon(P),** *Hyparrhenia lintonii(P), Mariscus macropus(P),* **Microchloa kunthii(P),** **Pennisetum mezianum(P),** **Sporobolus discosporus(P),** *Tephrosia pumila(F), Themeda triandra(P)*	
Setaria (KIL1E)	*Ischaemum brachyatherum(P), Orthosphon parvifolius(F),* **Pennisetum mezianum(P),** **Rhynchosia minima(F),** **Setaria trinervia(P)**	95 % - *Setaria trinervia* (P)
Setaria (KIL2D)	**Digitaria macroblephara(P),** *Ischaemum brachyatherum(P),* **Orthosphon parvifolius(F),** *Pennisetum mezianum(P), Rhynchosia minima(F),* **Setaria trinervia (P), Themeda triandra(P)**	95 % - *Setaria trinervia(P)*

Species with high relative frequency during all field campaigns are represented by bold; species life-form is represented by brackets (); P = perennial, A = annual, F = forbs.

4.1.2. Analysis of soil properties

Fig. 3 presents the results of soil physio-chemical characteristics for the grassland communities. First, we found the *Cynodon* community to have higher levels of OC (>1.9) at shallow depths as compared to other grassland communities with low levels of OC (<1.9) at all depths. Secondly, the single (KIL2D) co-occurrence (KIT1B) and the mixed (KIT1B, KIL1E, KIL1F) grassland communities had acidic soil levels (pH < 7.0). In contrast, the co-occurrence *Bothriochloa* and *Cynodon* (KIT1A), single dominance *Cynodon*, and mixed (KIL2C) had alkaline soil levels (pH > 7.0). Third, we found mixed (KIL1F) and *Cynodon* (KIL2A) communities to have high P concentration levels (ppm > 20) and moderate K concentration levels (between 110 and 250 mg/kg) at all depths compared to other grassland communities (P < 9 ppm, K < 110 ppm). Fourth, only the *Cynodon* (KIL2A) community contained moderate N levels (0.15 – 0.3 %), as compared to low levels (<0.15 %) for the other communities. Overall, we found that grassland communities with moderate to high levels of OC, P, N, and/or K content had a higher average Gcc than those

with low levels. The highest average Gcc was found for the *Cynodon* (KIL2A) community, and coincided with high levels of OC, P, K and N).

4.2. Animal frequency derived from phenocams

Fig. 4 shows an example frame with the animals detected using the MegaDetector RCNN model. Analysing the sampled frame images and comparing MegaDetector identification against the manual identification indicates that 87.15 % of the model variability is explained by the in-animal counts and an RMSE of 1.157 (see Supplementary Fig. S2). Furthermore, we found the detection confidence level was greater than 60 %. Finally, wet weather hindered accurate identification due to mist and water droplets on the camera lens, while warm and sunny conditions were the best.

4.3. Grassland variation derived from phenocams

Fig. 5a depicts the time series of grassland greenness as determined by the Green Chromatic Coordinate (Gcc) for all seven grassland communities from the end of March to the end of July 2019. The time-series profile and rates of green-up and senescence differed between grass communities. Three grassland communities had two distinct peaks in greenness during the period, with Gcc troughs by late May and early June. Co-occurrence *Bothriochloa and Cynodon* (KIT1A) and single dominance *Cynodon* (KIL2A) communities had the most pronounced mid and end season Gcc drops, with less prominent drops for the co-dominant (KIT1B) and mixed (KIL1F and KIL2C) communities. Additionally, our data shows that the Gcc levels for *Setaria* (KIL1E and KIL2D) community were the lowest. Overall, we found co-dominant (Kit1B) and mixed (KIL1F and KIL2C) communities to have greenness profiles that were generally similar, greening up in early May and senescing in mid-June.

4.4. Analysis of precipitation and air temperature

The corresponding PRCP and AT observations are shown in Fig. 5b. First, PRCP shows two significant episodes of higher precipitation, i.e., in late April and early June. The highest daily cumulative PRCP was 53.6 mm on 24 April during the first episode and 24.9 mm on 2 June during the second PRCP episode. Furthermore, our data show a single PRCP event of 9.4 mm recorded on 18 May. Following the first PRCP in late April, we observed a green-up phase for all seven grasslands communities, with the most rapid increases in the co-occurrence *Bothriochloa and Cynodon* (KIT1A) and single dominance *Cynodon* (KIL2A) communities. Here, Gcc drops in mid-May for the co-occurrence *Bothriochloa and Cynodon* (KIT1A), single dominance *Cynodon* (KIL2A) and mixed (KIL2C) communities, followed by a second PRCP episode in early June, resulting in a secondary green-up peak by mid-June.

The AT is variable throughout the season, with the value (27.77°) recorded on 23 June and the lowest (18.19°) on 24 May. Across the study period, the highest AT occurred on average on dry days and lower AT's on wet days, even though lower AT is also found during the dry early July.

4.5. Drivers of grassland dynamics

4.5.1. Site-level greenness and grazing intensity

Fig. 6 compares the Gcc time series to that of animal grazing. Panels a, b, c, and d depict transect 1, while panels e, f, and g depict transect 2. Both Gcc and animal counts fluctuate strongly during the period. For example, we find moderate to low animal grazing in mixed and co-occurrence *Bothriochloa and Cynodon* (KIT1A, KIT1B, and KIL1F) and *Setaria* (KIL1E) grassland communities along transect 1. Similarly, we find a gradual increase in grazing animals from the single dominance *Setaria* (KIL2D) to *Cynodon* (KIL2A) grassland communities. The *Cynodon* (KIL2A) community has the highest grazing animals among the two
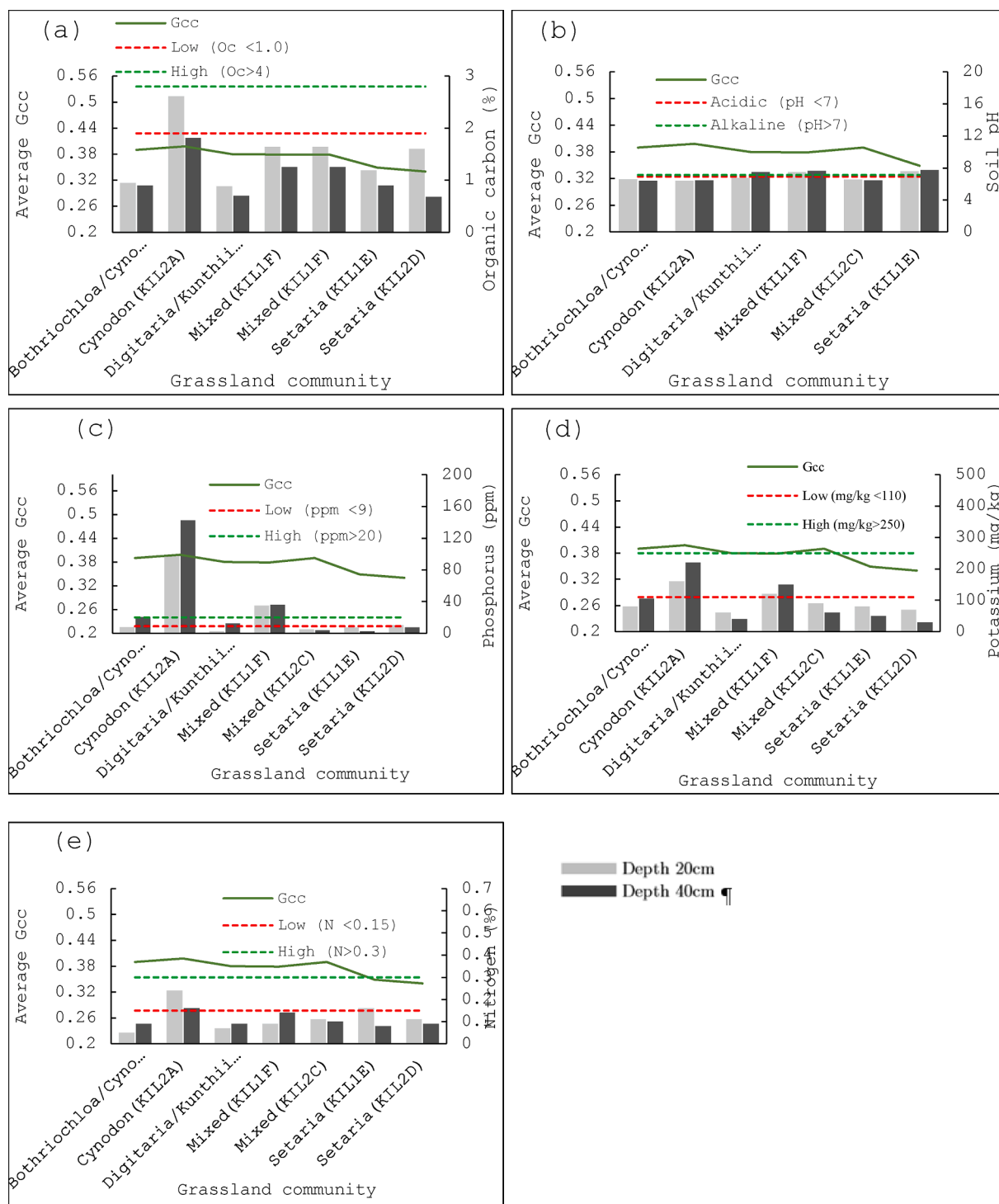
Fig. 3. Soil physio- chemical characteristics at the seven field sites; (a) Organic carbon; (b) Alkalinity - pH; (c) Phosporous; (d) Potassium; (e) Nitrogen.

transects, and also the highest overall Gcc levels. In addition, our findings show that the low Gcc levels for the *Setaria* (KIL1E and KIL2D) communities correspond to fewer grazing animals. However, these communities show an increase in animal grazing during the early green-up (see Fig. 6c and 6 g). Our results show a large variability in animal grazing pressure among the different grassland communities.

4.5.2. Quantitative assessment of drivers

We first estimated the single variable correlations with lags. Table 4 displays the lag correlation results between Gcc and PRCP, AT, and A.

Many grassland sites respond positively to PRCP, with an optimal lag of four days, with single occurence *Cynodon* (KIL2A) and co-occurence *Bothriochloa* and *Cynodon* (KIT1A) communities showing the most significant correlation coefficient of 0.72 and 0.75, respectively. *Setaria* community (KIL2D), on the other hand, had a longer lag, corresponding to 36 days, at a moderate correlation strength of 0.58. *Digitaria/Kunthii* (KIT1B) and *Setaria* (KIL1E) community data show no significant correlation strength for the PRCP variable.

The lag correlation results between Gcc and AT show that only the co-occurrence *Bothriochloa/Cynodon* (KIT1A), and mixed (KIL1F and
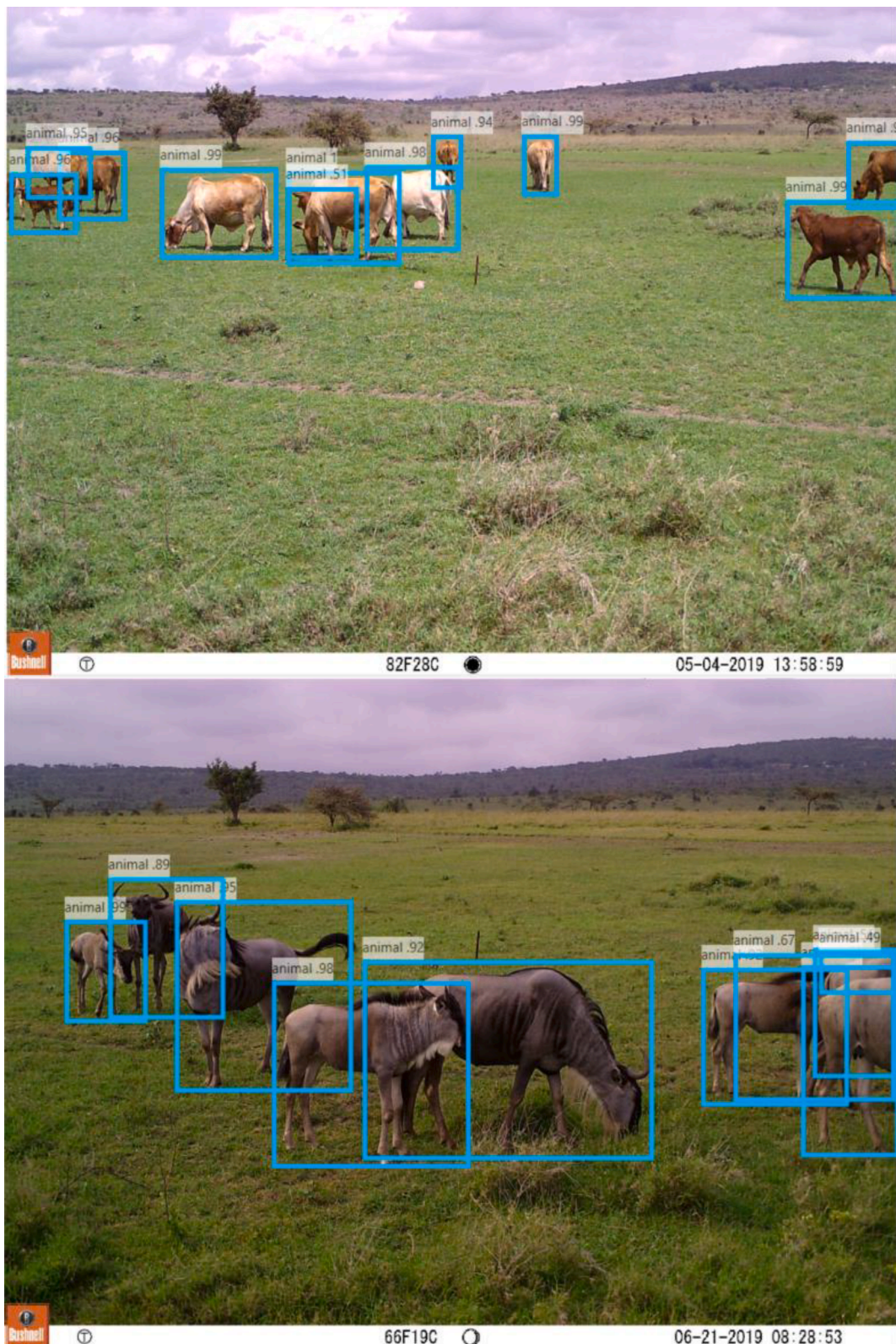
Fig. 4. Sample frames showing MegaDetector identification for the *Cynodon* (KIL2A) grassland community. The top panel shows livestock detection and the bottom panel wildlife detection. The blue squares indicate the single animals that were retrieved, and the confidence score is highlighted in white.

KIL2C) communities had a significant negative correlation (0.73, 0.60, and 0.59, respectively).

The lag correlation between Gcc and A shows that the animal response to changes in greenness varies across grassland communities. We found that the Gcc range had a poor correlation to A ranging from

−0.50 to 0.65, with no significance for *Digitaria/Kunthii* (KIT1B) and *Setaria* (KIL1E) communities. However, at the *Setaria* (KIL2D) community, we found a strong positive correlation between Gcc and A that corresponded to 12 days. Conversely, only *Cynodon* (KIL2A) showed a negative correlation (-0.50) between Gcc and A, with a lag of four days.
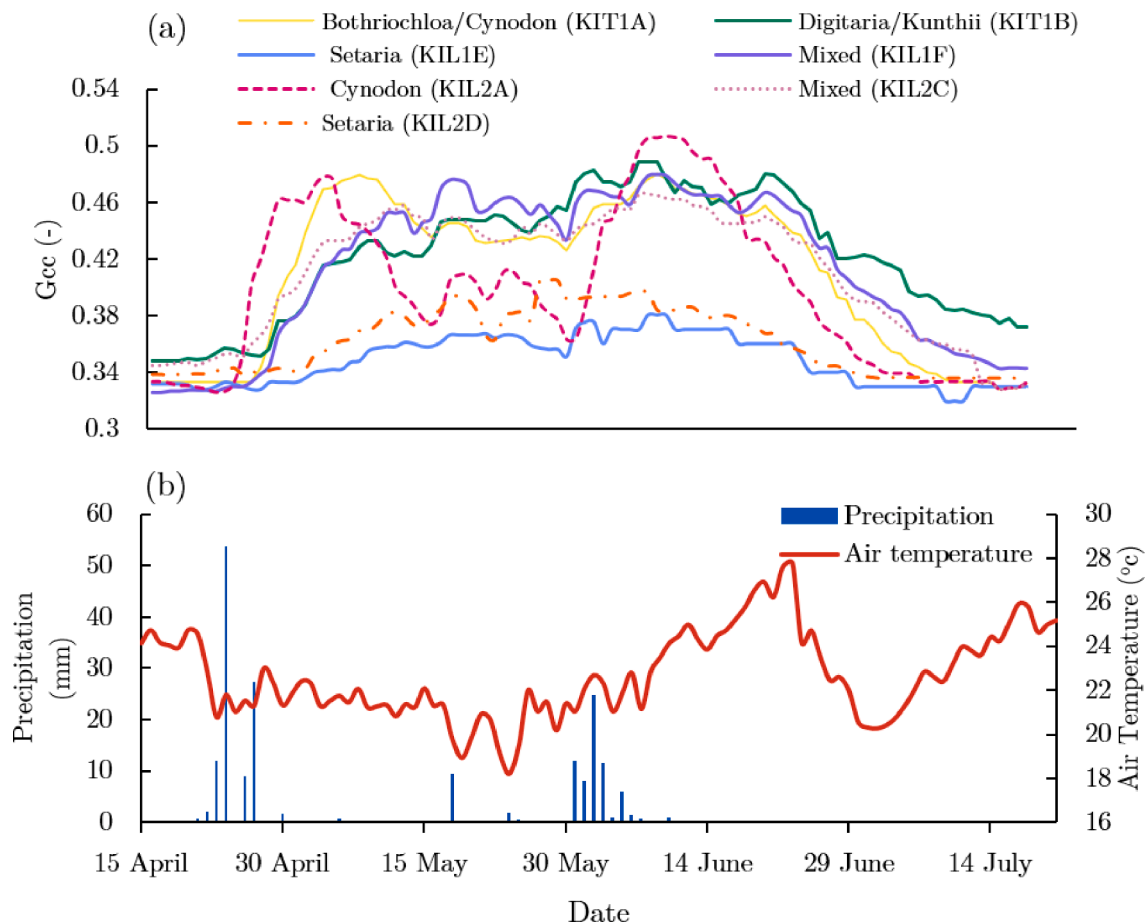
Fig. 5. (a) Seasonal Gcc phenology profiles for all the grassland communities; and (b) daily accumulation and mean for precipitation (mm) and air temperature (°C), respectively, for the study period.

Overall, our data show that mixed (KIL1F and KIL2C), and *Bothriochloa/Cynodon* (KIT1A), had a significant correlation (p < 0.05) with PRCP, AT, and A. *Digitaria/Kunthii* (KIT1B) and *Setaria* (KIL1E) communities showed no significant correlation with any of the variables.

Table 5 shows the results of the multivariate regression models for the seven grassland communities linking PRCP, AT, and A to greenness (see Supplementary Table S1 for the results of the Shapiro-Wilk normality test and multicollinearity results). Models 1–4 represent the various multi-variable combinations for the season (i.e., model 1 - PRCP and AT; model 2 - AT and A; model 3 - PRCP and A; model 4 - PRCP, AT and A).

A comparison of regression results across the study area shows that many models produced significant (p < 0.05) results for single dominance *Cynodon* (KIL2A), *Setaria* (KIL2D), co-occurrence *Bothriochloa/Cynodon* (KIT1A), and mixed (KIT1B, KIL1F and KIL2C) communities. However, the *Setaria* (KIL1E) community models were not significant, indicating that the Gcc variability could not be explained by this site's combined PRCP, AT, and A variability. Comparing the adjusted R-squared for all the models across the study area indicates that models 1 (PRCP and AT) contributed the most to Gcc in *Bothriochloa/Cynodon* (KIT1A), with an adjusted R^2 − 0.75. In contrast, model 2 (AT and A) contributed the most to Gcc in *Digitaria/Kunthii* (KIT1B), mixed (KIL1F), and *Setaria* (KIL2D) communities, with an adjusted R^2 of 0.30, 0.45 and 0.47, respectively. Furthermore, models 3 (PRCP and A) contributed the most to Gcc in *Cynodon* (KIL2A) community, with an adjusted R^2 − 0.56, while model 4, which includes all three predictor variables (PRCP, AT, and A), indicates the contribution of all the variables to Gcc in mixed (KIL2C) community with an adjusted R^2 − 0.57. Overall, PRCP played a role in three of the grasslands (*Cynodon* (KIL2A), *Bothriochloa/Cynodon*

(KIT1A), and mixed (KIL2C)), AT in five (*Bothriochloa/Cynodon* (KIT1A), *Digitaria/Kunthii* (KIT1B) mixed (KIL1F, KIL2C), and *Setaria* (KIL2D)), and A also in five (*Digitaria/Kunthii* (KIT1B). mixed (KIL1F, KIL2C), *Cynodon* (KIL2A), and *Setaria* (KIL2D)) communities. Overall, only for three sites greater than 50 % of the Gcc variability could be explained from PRCP, AT, and A. Similarly, the drivers' contribution per grassland community are given in Fig. S1, with PRCP contributing most to *Cynodon* and *Bothriochloa/Cynodon* communities, AT contributing most to *Bothriochloa/Cynodon* and Highly-diverse mixed communities, and grazing contributing most to both *Setaria* communities and the *Digitaria/Kunthii* community.

5. Discussion

5.1. Drivers of grassland variation

Precipitation, temperature, and grazing influence grassland community greenness, albeit at different times. Precipitation is associated with early-season community grass flushing, temperature increases influence community grass senescence, and heavy grazing is associated with mid-season losses in community grass greenness. Using multivariate regressions (Table 5), the inclusion of AT to PRCP or A to AT explains marginally better the variability in greenness for various grassland communities in semi-arid Kenya. These findings support previous research on the role of precipitation, temperature, and grazing in the structural dynamics of grasslands (D'Adamo et al., 2021; Liu et al., 2021; Tong et al., 2019). However, this study provides new evidence of the association of precipitation, temperature and grazing drivers on the production of grasses in single, co-dominant, and mixed-species
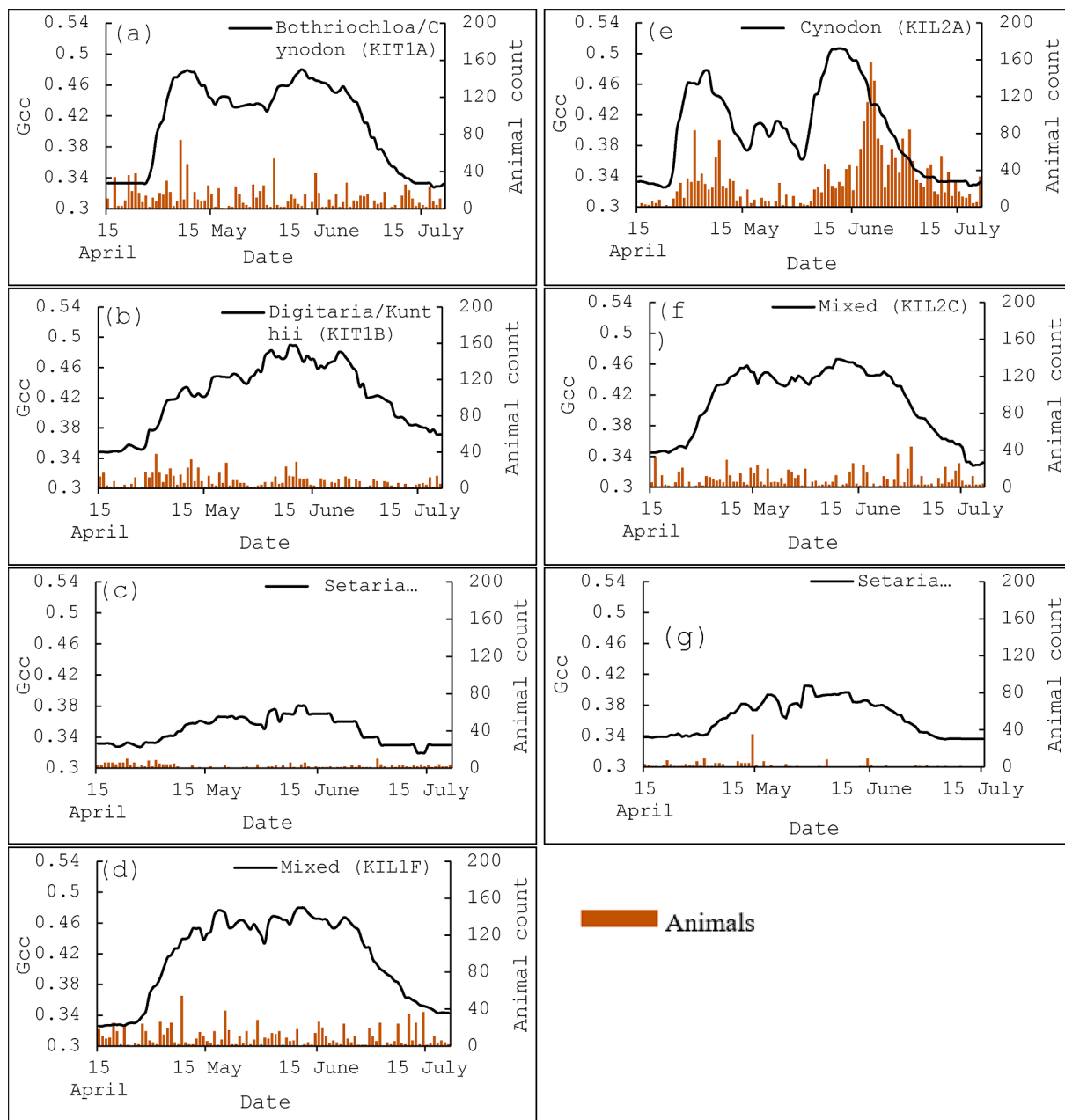
Fig. 6. Time-series of Gcc for each grassland community and derived animal counts across the season. Transect 1 is represented by grassland site a, b, c and d for KIT1A, KIT1B, KIL1E and KIT1F, respectively, whereas transect 2 by e, f, and g for KIL2A, KIL2C and KIL2D, respectively.

communities.

Our study quantifies how the three drivers precipitation, air temperature and grazing do not impact grassland species communities uniformly. Precipitation and grazing were found to be significantly (adjusted R^2 0.56) associated with the variability in the greenness of the *Cynodon* community (KIL2A). Specifically, precipitation rapidly (4 days) increased *Cynodon* community green-up (see Fig. 5). In contrast, animal grazing was associated with the loss in community grass greenness during the mid-season. These results confirm the association between precipitation and grazing as essential drivers of temporal variability in grasslands (Hoffmann et al., 2016; Liu et al., 2019a) and also confirm a strong presence of grazing in *Cynodon* communities.

There are several possible explanations for the result. First, *Cynodon's* well-developed rhizomes and stolons can facilitate the absorption of water and soil nutrients, and help explain the plant's rapid reaction to water availability following the early-season rainfall events. Using its

well-formed root systems, *Cynodon* has been shown to withstand drought and other disturbances and rebound quickly following water influxes into the system due to its rhizome survival during dry months (Holm et al., 1977; Mureithi et al., 2016). Secondly, the high grazing intensity may be explained by the palatability and productivity of the *Cynodon* community. Indeed, *Cynodon* is a highly palatable and nutritious grass species that encourages herbivory, resulting in trampling and defoliation (Dalle, 2020; Mureithi et al., 2016; Ondier et al., 2019). The mid-season decline in the *Cynodon* community greenness is consistent with literature describing the impact on grass defoliation shortly after animal trampling and grazing (Li et al., 2019; Watson et al., 2019). Finally, we found high organic carbon, phosphorus, potassium, and nitrogen levels in the *Cynodon* community soils (Fig. 3), which point to good soil conditions that favour root development and moisture retention (Leghari et al., 2016; Prajapati & Modi, 2012; Raghothama, 2015).

Additionally, in the *Bothriochloa/Cynodon* co-occurrence grassland

Table 4

Pearson correlation coefficients between Gcc and lagged precipitation, air temperature and animal frequency. Each lag represents four days.

Variables	Grassland community	Lags									
		0	1	2	3	4	5	6	7	8	9
PRCP	*Bothriochloa/Cynodon* (KIT1A)	0.53	**0.72**[**]	0.15	0.01	0.1	−0.24	−0.53	−0.09	−0.01	0.16
	Cynodon (KIL2A)	0.64	**0.75**[**]	0.17	−0.13	−0.23	−0.32	−0.23	−0.09	−0.3	0.07
	Digitaria/Kunthii (KIT1B)	0.19	0.38	−0.02	−0.14	0.15	−0.07	−0.47	0.02	0.22	0.36
	Mixed (KIL1F)	0.2	**0.58**[*]	0.09	0.1	0.25	−0.05	−0.33	0.06	−0.02	0.09
	Mixed (KIL2C)	0.47	**0.55**	0.31	−0.13	0.13	−0.17	−0.5	−0.21	0.19	0.08
	Setaria (KIL1E)	0.13	0.29	−0.16	0.01	−0.29	−0.06	−0.28	−0.29	−0.12	0.47
	Setaria (KIL2D)	−0.02	0.23	0.34	−0.15	−0.23	−0.29	−0.35	0.06	**0.58**[*]	−0.24
AT	*Bothriochloa/Cynodon* (KIT1A)	−0.13	−0.46	−0.65	**−0.73**[**]	−0.57	−0.28	−0.12	−0.06	0.2	0.46
	Cynodon (KIL2A)	−0.16	−0.25	−0.32	−0.36	−0.27	−0.09	−0.03	0.06	0.22	0.27
	Digitaria/Kunthii (KIT1B)	−0.2	−0.3	−0.29	−0.35	−0.33	−0.25	−0.09	−0.08	0.11	0.18
	Mixed (KIL1F)	−0.08	−0.25	−0.41	−0.53	**−0.60**[*]	−0.45	−0.22	−0.13	0.19	0.31
	Mixed (KIL2C)	−0.04	−0.17	−0.39	−0.56	**−0.59**[*]	−0.46	−0.22	0.05	0.09	0.46
	Setaria (KIL1E)	0.14	−0.1	−0.39	−0.34	−0.13	0.16	0.25	0.21	0.35	0.07
	Setaria (KIL2D)	−0.2	−0.51	−0.45	−0.24	−0.19	0.01	0.09	0.24	0	0.68
A	*Bothriochloa/Cynodon* (KIT1A)	0.27	0.36	−0.03	−0.05	0.14	0.09	0.13	0.38	**0.56**[*]	0.05
	Cynodon (KIL2A)	−0.49	**−0.50**[*]	−0.39	−0.28	−0.13	−0.07	0.07	0.25	0.41	0.5
	Digitaria/Kunthii (KIT1B)	0.05	−0.34	0.34	0.08	0.1	0.19	0.24	0.56	−0.01	−0.09
	Mixed (KIL1F)	0.05	0.22	−0.01	−0.08	0.28	0.27	0.01	−0.11	**0.51**[*]	−0.06
	Mixed (KIL2C)	−0.3	−0.27	0.13	0.21	−0.11	0.34	**0.50**[*]	−0.07	0.07	−0.17
	Setaria (KIL1E)	−0.2	0.12	−0.08	0.32	−0.1	−0.11	−0.08	0.25	0.19	0.42
	Setaria (KIL2D)	−0.13	0.06	0.02	**0.65**[*]	−0.15	0.11	0.41	0.25	−0.08	−0.02

[**]=p < 0.01; [*]= ρ < 0.05; PRCP- Precipitation accumulation lag, AT – average Air temperature lag,
A – Animals frequency accumulation count.

community, we found temperature and precipitation to be significantly associated with grass productivity (adjusted R^2 0.75) but not herbivory. Although animals were present at this site throughout the season (Fig. 6a), *Bothriochloa* species are not highly regarded by grazers, especially with increased age (Skerman & Riveros, 1990). Also, *Bothriochloa* species are impacted by increases in temperature as they can only tolerate drought for short periods (Heuzé et al., 2016). This may result in mid-season declines in *Bothriochloa* greenness (Fig. 6a). The rapid greenup following the season's first rains, similar in magnitude to the *Cynodon* dominated community (Fig. 5a), can be attributed to the presence of *Cynodon* in the community.

Another important finding was that the *Setaria* community showed lower greenness levels when compared to other grassland communities, and the greenness variability is only weakly driven by precipitation and grazing (see Fig. 5 and Table 5). *Setaria trinervia* is a perennial grass species with long stems and bristle spikelets with less leafy green material. Vrieling et al. (2018) suggest that the reduced greenness observed by cameras can also result from non-photosynthetic elements (stems, seed heads) on plant tops. Consequently, *Setaria* is a highly palatable species when young, but due to the stem dominance and low foliage later in the season, it loses preference for grazing (Skerman & Riveros, 1990). The finding is consistent with those of Ondier et al. (2019), who found that reduced grazing disturbance allows a few plant species to become dominant and develop large populations with high biomass. *Setaria* is known to tolerates flooding, dry condotions and poor clay soils where it can spread if seeding takes place (Skerman & Riveros, 1990).

In the *Digitaria/Kunthii* co-occurrence grassland community, we found no association with precipitation, temperature and grazing. *Digitaria* species require adequate rich soils and moisture levels greater than 500 mm (FAO, 2012) for growth which may explain the lack of association with precipitation given the low soil organic carbon, nitrogen, potassium and phosphorus in this community (see Fig. 3). *Kunthii* is a short, clustered grass species which can grown in shallow hardpan soils (Glover et al., 1964), and may be less rapidly influenced by precipitation buildup. The lack of association with grazing may be the result of moderate to low palatability of *Digitaria/Kunthii* community (Jawuoro et al., 2017; Skerman & Riveros, 1990), especially at the green-up phase. Also, as earlier noted, occurrence of *Bothriochloa* species (see Table 3) in the community could be a deterrent for the grazing animals. Interestingly, the *Digitaria/Kunthii* community has the highest greenness and

shallowest decrease in the late season senescence phase (Fig. 4a), which may explain the lack of association with temperature.

Mixed communities (KIL1F/KIL2C) with high species richness (Table 2) were associated with precipitation and temperature, and were also positively associated with moderate intensity grazing. The rapid greenup following precipitation in some of the species is a result of the growth of ephemerals grass species (Jawuoro et al., 2017) such as *Pennisetum* species. Ephemerals are grass species with rapid growth following precipitation event (Lugusa et al., 2016). Interestingly, in the mixed communities of this study, we found variability in greenness to be associated with the marginal herbivore activities (see Fig. 6b, d, and f also Table 4, 5). The marginal grazing intensity here may help to explain the species richness, diversity, and evenness (see Table 2). Marginal grazing intensity grazing sets up an environment that encourages grassland reproduction and plant diversity (Mureithi et al., 2010; Jawuoro et al., 2017) through growth of forbs in Kenya, while heavy grazing can reduce the density of selected species while promoting the growth of non-palatable forbs' (Jacobs & Naiman, 2008; Todd, 2006).

5.2. Limitations and future directions

Grassland species composition, weather drivers, and grazing intensity accounted for slightly more than 50 % of our study area's spatial and temporal variation. However, there is still much-unexplained variability in grassland productivity, which may be explained by the complex interactions between the various drivers and other factors that this work could not assess, such as terrain characteristics and plant functional traits (growth form, water flux and below ground storage organs). For example, topography influences species diversity and available soil moisture (Gong et al., 2008), and plant functional traits (competition and growth rate) affect variability in vegetation among species (König et al., 2018). Thus it makes real-world dynamics challenging to model and limits our complete understanding of these complex interactions.

The interaction of grassland communities, weather drivers and herbivory through grazing by wildlife and livestock is complex. While we attempted to unravel some of these interactions here, we also note that these are site-specific and depend on various factors such as species composition and weather drivers. Moreover, we acknowledge that our grassland communities likely do not represent all variability within drylands and possibly even within the Kapiti grasslands. Also, only one

Table 5

Regression analysis of Gcc and variable predictors of precipitation, land surface temperature, and animal frequency.

Transect	Grassland community	model	Formula	Adjusted R^2
1	*Bothriochloa/ Cynodon* (KIT1A)	1	Gcc = 0.051 + 0.0005PRCP** − 0.002AT**	**0.75****
		2	Gcc = 0.056–0.003AT** + 0.0002A **	**0.74****
		3	Gcc = − 0.004 + 0.0009PRCP* − 0.0001A	**0.45***
		4	Gcc = 0.052 + 0.0003PRCP − 0.003AT** − 0.0001A	**0.74****
	Digitaria/ Kunthii (KIT1B)	1	Gcc = 0.023 + 0.0001PRCP − 0.001AT	0.08
		2	Gcc = 0.015–0.001AT − 0.0003A*	**0.30***
		3	Gcc = − 0.014 + 0.0001PRCP − 0.0001A	0.29
		4	Gcc = 0.012 + 0.0001PRCP − 0.001AT − 0.0001A	0.25
(KIL1E)	*Setaria*	1	Gcc = 0.019 + 0.0001PRCP − 0.0001AT	0.05
		2	Gcc = 0.009–0.001AT + 0.0001A	0.07
		3	Gcc = − 0.005 + 0.0001PRCP + 0.0001A	0.05
		4	Gcc = 0.009 + 0.0001PRCP − 0.001AT + 0.0001A	0.01
	Mixed (KIL1F)	1	Gcc = 0.034 + 0.0001PRCP − 0.001AT	**0.42***
		2	Gcc = 0.036–0.002AT* − 0.0001A	**0.45****
		3	Gcc = − 0.011 + 0.0004PRCP − 0.0001A	**0.28***
		4	Gcc = 0.031 + 0.0001PRCP − 0.002AT* − 0.0001A	**0.45***
2	*Cynodon* (KIL2A)	1	Gcc = 0.0152 + 0.002PRCP** − 0.001AT	**0.50****
		2	Gcc = 0.035–0.001AT − 0.0001A	0.14
		3	Gcc = − 0.004 + 0.001PRCP** − 0.0001A	**0.56****
		4	Gcc = − 0.008 + 0.001PRCP** − 0.0001AT − 0.000A	**0.53****
	Mixed (KIL2C)	1	Gcc = 0.034 + 0.000PRCP − 0.002AT	**0.40***
		2	Gcc = 0.038–0.002AT** + 0.0002A *	**0.54****
		3	Gcc = − 0.014 + 0.0004PRCP − 0.0002A	**0.36***
		4		**0.57***

Table 5 (*continued*)

Transect	Grassland community	model	Formula	Adjusted R^2
	Setaria (KIL2D)	1	Gcc = 0.030 + 0.0002PRCP − 0.002AT* − 0.0002A*	0.28
		1	Gcc = 0.018 + 0.0001PRCP − 0.001AT	
		2	Gcc = 0.024–0.001AT + 0.0005A *	**0.47***
		3	Gcc = − 0.006 + 0.0001PRCP − 0.0001A	**0.36***
		4	Gcc = 0.023 + 0.0001PRCP − 0.001AT − 0.0001A	**0.41***

PRCP– Precipitation; AT – air temperature; A – Animal frequency; *= $\rho < 0.05$, **= $\rho < 0.01$ and is highlighted in bold.

weather station was used in the study, and we hypothesise that local climate varies across spatial scales influencing species diversity. Nevertheless, our approach has demonstrated the ability to capture these fine-scale spatial and temporal variability and helps replicate in more locations to understand the complexities better.

The relatively inexpensive camera traps have enormous potential to support dryland monitoring as they look at the temporal and spatial variability in these heterogeneous dryland systems. Compared to the phenological Webcam, that often requires an internet connection and is expensive to set up, especially for less developed countries with poor broadband connectivity. Because they are cheaper, multiple camera traps could be used instead of a single phenology webcam to get a broader range of samples for about the same amount of resources. Our study demonstrated that the low-cost camera systems provided comparable data to gain insights into the spatial and temporal grasslands dynamics. These findings are consistent with previous research highlighting the potential of inexpensive camera technology to support ecological monitoring (Cheng et al., 2020; Vrieling et al., 2018).

Finally, in this study, we have successfully demonstrated how the pre-trained RCNN machine learning model can be used to estimate the grazing intensity of wildlife and livestock based on digital repeat photographs of single frames. In addition, we found the animal count based on the RCNN to be consistent with the manual count with an R^2 of 87 % (see supp. Mat. Fig. 2). Our findings show comparable results with other studies of greater than 80 % detection (Beery et al., 2019; Carl et al., 2020; Norouzzadeh et al., 2018). For example, Carl et al. (2020) achieved a detection accuracy of 94 % using a combination of Faster RCNN and Inception ResNet V2 pre-trained computer vision models to automatically detect wild mammals in Europe. However, more research is required to address the limitations of poor animal detection in a high animal density frame. Also, in this study, for simplicity, we ignored the multispecies (wildlife and livestock) images and considered them all like animals. Future studies could determine how wildlife and livestock drive grassland variability by undergoing fine-scale herbivory characterization. Such information is vital in rangeland management, especially in deciding the grassland productivity and carrying capacity.

6. Conclusion

This study demonstrated the potential of using low-cost digital repeat photography to assess the fine-scale spatial and temporal patterns of grassland dynamics in a heterogeneous semi-arid grassland influenced by grassland species communities, weather and grazing factors. Although a substantial amount of greenness variability remains unexplained, precipitation, temperature, and grazing are shown to influence grassland community greenness, albeit at different times. For example,

precipitation is associated with early-season community grass flushing, temperature influences community grass senescence, and heavy grazing is associated with mid-season community grass greenness losses. The *Cynodon* communities are affected by precipitation and herbivory, while the co-occurrence *Bothriochloa/Cynodon* communities have precipitation and temperature, and *Setaria* communities have temperature and grazing as the main driver. This study's technological application of the low-cost camera systems demonstrates how it adds value by providing temporal dynamics, spatial variability, and estimation of grazing regimes. Our study is not conclusive about the drivers of semi-arid grassland dynamics but rather demonstrates the complexity of interactions in these drylands and emphasizes their importance for designing more effective grassland management strategies.

Funding

CRediT authorship contribution statement

James M. Muthoka: Conceptualization, Data curation, Formal analysis, Visualization, Investigation, Methodology, Software, Validation, Writing – original draft, Writing – review & editing. **Alexander S. Antonarakis:** Supervision, Writing – review & editing. **Anton Vrieling:** Supervision, Writing – review & editing. **Francesco Fava:** Supervision, Writing – review & editing. **Edward E. Salakpi:** Software, Data curation. **Pedram Rowhani:** Supervision, Writing – review & editing.

Declaration of Competing Interest

The authors declare the following financial interests/personal relationships which may be considered as potential competing interests: James M. Muthoka reports financial support was provided by NERC Science for Humanitarian Emergencies and Resilience Studentship Cohort (SHEAR SSC). James M. Muthoka reports financial support was provided by SHEAR ForPAc project.

Data availability

Data to this article can be found online at http://doi.org/10.25377/sussex.20390511.

Acknowledgements

Appendix A. Supplementary data

Supplementary data to this article can be found online at https://doi.org/10.1016/j.ecolind.2022.109223.

References

Akwee, P.E., Palapala, V.A., Gweyi-Onyango, J.P., 2017. A comparative study of plant species composition of grasslands in Saiwa Swamp National Park and Kakamega Forest, Kenya. Kamla Raj Enterprises 1 (2), 77–83. https://doi.org/10.1080/09766901.2010.11884719.

Ali, I., Cawkwell, F., Dwyer, E., Barrett, B., Green, S., 2016. Satellite remote sensing of grasslands: from observation to management. J. Plant Ecol. 9 (6), 649–671. https://doi.org/10.1093/jpe/rtw005.

Beery, S., Wu, G., Rathod, V., Votel, R., & Huang, J., 2019. Context R-CNN: Long Term Temporal Context for Per-Camera Object Detection. Proceedings of the IEEE Computer Society Conference on Computer Vision and Pattern Recognition, 13072–13082. http://arxiv.org/abs/1912.03538.

Bengtsson, J., Bullock, J.M., Egoh, B., Everson, C., Everson, T., O'Connor, T., O'Farrell, P. J., Smith, H.G., Lindborg, R., 2019. Grasslands-more important for ecosystem services than you might think. Ecosphere 10 (2), e02582.

Boval, M., Dixon, R.M., 2012. The importance of grasslands for animal production and other functions: a review on management and methodological progress in the tropics. Animal 6 (5), 748–762. https://doi.org/10.1017/S1751731112000304.

Braun-blanquet, J., 1932. Plant sociology. The study of plant communities. First ed. Plant Sociology. The Study of Plant Communities. First Ed.

Caparros-Santiago, J.A., Rodriguez-Galiano, V., Dash, J., 2021. Land surface phenology as indicator of global terrestrial ecosystem dynamics: A systematic review. ISPRS J. Photogramm. Remote Sens. 171, 330–347. https://doi.org/10.1016/j.isprsjprs.2020.11.019.

Carl, C., Schönfeld, F., Profft, I., Klamm, A., Landgraf, D., 2020. Automated detection of European wild mammal species in camera trap images with an existing and pre-trained computer vision model. Eur. J. Wildl. Res. 66 (4), 62. https://doi.org/10.1007/s10344-020-01404-y.

Caroline King-Okumu, B., Vivian Wasonga, O., Yimer, E., 2015. Pastoralism pays: new evidence from the Horn of Africa 1. http://pubs.iied.

Cheche, W.W., Githae, E.W., Omondi, S.F., Magana, A.M., 2015. An inventory and assessment of exotic and native plant species diversity in the Kenyan rangelands: case study of Narok North Sub-County. J. Ecol. Natural Environ. 7 (8), 238–246.

Cheng, Y., Vrieling, A., Fava, F., Meroni, M., Marshall, M., Gachoki, S., 2020. Phenology of short vegetation cycles in a Kenyan rangeland from PlanetScope and Sentinel-2. Remote Sens. Environ. 248, 112004 https://doi.org/10.1016/j.rse.2020.112004.

Chytrý, M., Tichý, L., Chytrý, M., Tichý, L., 2003. Diagnostic, constant and dominant species of vegetation classes and alliances of the Czech Republic: a statistical revision. In Folia Sci. Nat. Univ. Masaryk. Brun. (Vol. 108). Masaryk University Brno. http://www.botanickafotogalerie.cz/diagnostic_species.pdf.

D'Adamo, F., Ogutu, B., Brandt, M., Schurgers, G., Dash, J., 2021. Climatic and non-climatic vegetation cover changes in the rangelands of Africa. Global Planet. Change 202, 103516. https://doi.org/10.1016/j.gloplacha.2021.103516.

Dalle, G., 2020. Evaluation of forage quantity and quality in the semi-arid Borana Lowlands, Southern Oromiam, Ethiopia. Tropical Grasslands-Forrajes Tropicales 8 (2), 72–85. https://doi.org/10.17138/tgft(8)72-85.

Daoud, J.I., 2017. Multicollinearity and regression analysis. J. Phys. Conf. Ser. 949 (1), 012009 https://doi.org/10.1088/1742-6596/949/1/012009.

FAO. (2012). A searchable catalogue of grass and forage legumes. FAO, Rome, Italy. https://web.archive.org/web/20170120044942/http://www.fao.org/ag/AGP/AGPC/doc/GBASE/default.htm.

FAO. (2019). Standard operating procedure for soil organic carbon; Walkley-Black method Titration and colorimetric method. http://www.fao.org/3/ca7471en/ca7471en.pdf.

Fennell, M., Beirne, C., Burton, A. C., 2022. Use of object detection in camera trap image identification: assessing a method to rapidly and accurately classify human and animal detections for research and application in recreation ecology. BioRxiv, 2022.01.14.476404. doi: 10.1101/2022.01.14.476404.

Filippa, G., Cremonese, E., Migliavacca, M., Galvagno, M., Forkel, M., Wingate, L., Tomelleri, E., Morra di Cella, U., Richardson, A.D., 2016. Phenopix: A R package for image-based vegetation phenology. Agric. For. Meteorol. 220, 141–150. https://doi.org/10.1016/j.agrformet.2016.01.006.

Gareth, J., Witten, D., Hastie, T., Tibshirani, R., 2021. Linear Regression. In An Introduction to Statistical Learning (pp. 59–128). Springer US. doi: 10.1007/978-1-0716-1418-1_3.

Gillespie, A.R., Kahle, A.B., Walker, R.E., 1987. Color enhancement of highly correlated images. II. Channel ratio and "chromaticity" transformation techniques. Remote Sens. Environ. 22 (3), 343–365. https://doi.org/10.1016/0034-4257(87)90088-5.

Githae, E., 2018. Status of Opuntia invasions in the arid and semi-arid lands of Kenya. CAB Reviews: Perspectives in Agriculture, Veterinary Science, Nutrition and Natural Resources 13 (003), 1–7. https://doi.org/10.1079/PAVSNNR201813003.

Glover, P.E., Trump, E.C., Wateridge, L.E.D., 1964. Termitaria and Vegetation Patterns on the Loita Plains of Kenya. J. Ecol. 52 (2), 367. https://doi.org/10.2307/2257603.

Gómez-Giráldez, P.J., Pérez-Palazón, M.J., Polo, M.J., González-Dugo, M.P., 2020. Monitoring grass phenology and hydrological dynamics of an oak-grass savanna ecosystem using Sentinel-2 and terrestrial photography. Remote Sensing 12 (4), 600. https://doi.org/10.3390/rs12040600.

Gong, X., Brueck, H., Giese, K.M., Zhang, L., Sattelmacher, B., Lin, S., 2008. Slope aspect has effects on productivity and species composition of hilly grassland in the Xilin River Basin, Inner Mongolia, China. J. Arid Environ. 72 (4), 483–493. https://doi.org/10.1016/j.jaridenv.2007.07.001.

Gromping, U., 2006. Relative Importance for Linear Regression in R: the Package relaimpo. J. Stat. Softw. 17 (1), 1–27. https://doi.org/10.18637/jss.v017.i01.

Hennekens, S.M., Schaminée, J.H.J., 2001. TURBOVEG, a comprehensive data base management system for vegetation data. J. Veg. Sci. 12 (4), 589–591. https://doi.org/10.2307/3237010.

Heuzé, V., Thiollet, H., & Tran, G. (2016). *Creeping bluegrass (Bothriochloa insculpta)*. Feedipedia, a Programme by INRAE, CIRAD, AFZ and FAO. https://www.feedipedia.org/node/494.

Hoffmann, C., Giese, M., Dickhoefer, U., Wan, H., Bai, Y., Steffens, M., Liu, C., Butterbach-Bahl, K., Han, X., 2016. Effects of grazing and climate variability on grassland ecosystem functions in Inner Mongolia: Synthesis of a 6-year grazing experiment. J. Arid Environ. 135, 50–63. https://doi.org/10.1016/j.jaridenv.2016.08.003.

Holm, L.G., Plucknett, D.L., Pancho, J.V., Herberger, J.P., 1977. The world's worst weeds. University Press of Hawaii, Distribution and biology.

ILRI. (2019). Kapiti Research Station: A livestock, environmental and agricultural research station in southeastern Kenya. https://hdl.handle.net/10568/107222.

Jacobs, S.M., Naiman, R.J., 2008. Large African herbivores decrease herbaceous plant biomass while increasing plant species richness in a semi-arid savanna toposequence. J. Arid Environ. 72 (6), 891–903. https://doi.org/10.1016/j.jaridenv.2007.11.015.

Jawuoro, S.O., Koech, O.K., Karuku, G.N., Mbau, J.S., 2017. Plant species composition and diversity depending on piospheres and seasonality in the southern rangelands of Kenya. Ecological Processes 6 (1). https://doi.org/10.1186/s13717-017-0083-7.

Jonge, I.K., Veldhuis, M.P., Vrieling, A., Olff, H., 2022. Camera traps enable the estimation of herbaceous aboveground net primary production (<scp>ANPP</scp>) in an African savanna at high temporal resolution. Remote Sens. Ecol. Conserv. https://doi.org/10.1002/rse2.263.

Kioko, J., Kiringe, J.W., Seno, S.O., 2012. Impacts of livestock grazing on a savanna grassland in Kenya. J. Arid Land 4 (1), 29–35. https://doi.org/10.3724/SP.J.1227.2012.00029.

König, P., Tautenhahn, S., Cornelissen, J.H.C., Kattge, J., Bönisch, G., Römermann, C., 2018. Advances in flowering phenology across the Northern Hemisphere are explained by functional traits. Glob. Ecol. Biogeogr. 27 (3), 310–321. https://doi.org/10.1111/geb.12696.

Leghari, S.J., Wahocho, N.A., Laghari, G.M., HafeezLaghari, A., MustafaBhabhan, G., HussainTalpur, K., Bhutto, T.A., Wahocho, S.A., Lashari, A.A., 2016. Role of nitrogen for plant growth and development: a review. Adv. Environ. Biol. 10 (9), 209–219. https://go.gale.com/ps/i.do?p=AONE&sw=w&issn=19950756&v=2.1&it=r&id=GALE%7CA472372583&sid=googleScholar&linkaccess=fulltext.

Li, Y.u., Dong, S., Gao, Q., Zhang, Y., Liu, S., Swift, D., Ganjurjav, H., Hu, G., Wang, X., Yan, Y., Wu, H., Luo, W., Ge, Y., Li, Y., Zhao, Z., Gao, X., Li, S., Song, J., Collins, B., 2019. The effects of grazing regimes on phenological stages, intervals and divergences of alpine plants on the Qinghai-Tibetan Plateau. J. Veg. Sci. 30 (1), 134–145.

Linderman, M., Zeng, Y., Rowhani, P., 2010. Climate and land-use effects on interannual fAPAR variability from MODIS 250 m data. Photogramm. Eng. Remote Sens. 76 (7), 807–816.

Liu, Y., Wang, Q., Zhang, Z., Tong, L., Wang, Z., Li, J., 2019. Grassland dynamics in responses to climate variation and human activities in China from 2000 to 2013. Sci. Total Environ. 690, 27–39. https://doi.org/10.1016/J.SCITOTENV.2019.06.503.

Liu, Y., Yang, P., Zhang, Z., Zhang, W., Wang, Z., Zhang, Z., Ren, H., Zhou, R., Wen, Z., Hu, T., 2021. Diverse responses of grassland dynamics to climatic and anthropogenic factors across the different time scale in China. Ecol. Ind. 132, 108341 https://doi.org/10.1016/J.ECOLIND.2021.108341.

Lugusa, K.O., Wasonga, O.V., Elhadi, Y.A., Crane, T.A., 2016. Value chain analysis of grass seeds in the drylands of Baringo County, Kenya: a producers' perspective. Pastoralism 6 (1), 1–15. https://doi.org/10.1186/S13570-016-0053-1/FIGURES/8.

Matongera, T.N., Mutanga, O., Sibanda, M., Odindi, J., 2021. Estimating and monitoring land surface phenology in rangelands: a review of progress and challenges. Remote Sensing 13 (11), 2060. https://doi.org/10.3390/rs13112060.

Mganga, K.Z., Musimba, N.K.R., Nyariki, D.M., Nyangito, M.M., Mwang'ombe, A.W., 2015. The choice of grass species to combat desertification in semi-arid Kenyan rangelands is greatly influenced by their forage value for livestock. Grass Forage Sci. 70 (1), 161–167. https://doi.org/10.1111/gfs.12089.

Microsoft. (2020). AI for Earth camera trap image processing API. github. https://github.com/microsoft/CameraTraps/blob/main/megadetector.md.

Mire, S., 2017. The role of cultural heritage in the basic needs of East African Pastoralists. African Study Monographs. African Study Monographs 53 (Supplementary Issue), 147–157. https://doi.org/10.14989/218908.

Motsara, M. R., Roy, R. N., 2008. Guide to laboratory establishment for plant nutrient analysis (Vol. 19). Food and Agriculture Organization of the United Nations Rome. http://www.fao.org/3/i0131e/i0131e.pdf.

Mureithi, S.M., Verdoodt, A., Van Ranst, E., 2010. Effects and Implications of Enclosures for Rehabilitating Degraded Semi-arid Rangelands: Critical Lessons from Lake Baringo Basin, Kenya. In: Zdruli, P., Pagliai, M., Kapur, S., Faz Cano, A. (Eds.), Land Degradation and Desertification: Assessment, Mitigation and Remediation. Springer Netherlands, Dordrecht, pp. 111–129.

Mureithi, S.M., Verdoodt, A., Njoka, J.T., Gachene, C.K.K., Warinwa, F., Van Ranst, E., 2016. Impact of Community Conservation Management on Herbaceous Layer and Soil Nutrients in a Kenyan Semi-Arid Savannah. Land Degrad. Dev. 27 (8), 1820–1830. https://doi.org/10.1002/ldr.2315.

Muthoka, J., Salakpi, E., Ouko, E., Yi, Z.-F., Antonarakis, A.S., Rowhani, P., 2021. Mapping Opuntia stricta in the Arid and Semi-Arid Environment of Kenya Using Sentinel-2 Imagery and Ensemble Machine Learning Classifiers. Remote Sensing 13 (8), 1494. https://doi.org/10.3390/rs13081494.

Nicholson, S.E., 2014. A detailed look at the recent drought situation in the Greater Horn of Africa. J. Arid Environ. 103, 71–79. https://doi.org/10.1016/j.jaridenv.2013.12.003.

Norouzzadeh, M.S., Nguyen, A., Kosmala, M., Swanson, A., Palmer, M.S., Packer, C., Clune, J., 2018. Automatically identifying, counting, and describing wild animals in camera-trap images with deep learning. PNAS 115 (25), E5716–E5725. https://doi.org/10.1073/pnas.1719367115.

Norouzzadeh, M.S., Morris, D., Beery, S., Joshi, N., Jojic, N., Clune, J., Schofield, M., 2021. A deep active learning system for species identification and counting in camera trap images. Methods Ecol. Evol. 12 (1), 150–161.

Nyariki, D.M., Amwata, D.A., 2019. The value of pastoralism in Kenya: Application of total economic value approach. Pastoralism 9 (1), 1–13. https://doi.org/10.1186/S13570-019-0144-X/TABLES/10.

O'Mara, F.P., 2012. The role of grasslands in food security and climate change. Ann. Bot. 110 (6), 1263–1270. https://doi.org/10.1093/aob/mcs209.

Okalebo, J.R., Gathua, K.W., Woomer, P.L., 2002. Laboratory Methods of Soil And Plant Analysis: A Working Manual, second edition. Sacred Africa, Nairobi, p. 21.

Ondier, J.O., Okach, D.O., Onyango, J.C., Otieno, D.O., 2019. Interactive influence of rainfall manipulation and livestock grazing on species diversity of the herbaceous layer community in a humid savannah in Kenya. Plant Diversity 41 (3), 198–205. https://doi.org/10.1016/j.pld.2019.04.005.

Pei, Z., Fang, S., Yang, W., Wang, L., Wu, M., Zhang, Q., Han, W., Khoi, D.N., 2019. The relationship between NDVI and climate factors at different monthly time scales: A case study of grasslands in inner mongolia, China (1982–2015). Sustainability (Switzerland) 11 (24), 7243. https://doi.org/10.3390/su11247243.

Polley, H.W., Derner, J.D., Jackson, R.B., Wilsey, B.J., Fay, P.A., 2014. Impacts of climate change drivers on C4 grassland productivity: scaling driver effects through the plant community. J. Exp. Bot. 65 (13), 3415–3424. https://doi.org/10.1093/jxb/eru009.

Prajapati, K., Modi, H.A., 2012. The importance of potassium in plant growth–a review. Indian J. Plant Sci. 1 (02–03), 177–186.

Raghothama, K. G., 2015. Phosphorus and Plant Nutrition: An Overview. Phosphorus: Agriculture and the Environment, 353–378. doi: 10.2134/AGRONMONOGR46.C11.

Reid, R. S., Galvin, K. A., Kruska, R. S., 2008. Global Significance of Extensive Grazing Lands and Pastoral Societies: An Introduction. In Fragmentation in Semi-Arid and Arid Landscapes (Vol. 9781402049, pp. 1–24). Springer Netherlands. doi: 10.1007/978-1-4020-4906-4_1.

Reinermann, S., Asam, S., Kuenzer, C., 2020. Remote sensing of grassland production and management—a review. Remote Sensing 12 (12), 1949. https://doi.org/10.3390/rs12121949.

Republic of Kenya. (2012). Vision 2030 Development Strategy for Northern Kenya and other Arid Lands. In *Final Report* (Issue August). https://www.ndma.go.ke/index.php/resource-center/policy-documents/send/44-policy-documents/4300-vision-2030-development-strategy-for-asals.

Republic of Kenya. (2021). Range management and pastoralism strategy 2021-2031. https://www.iyrp.info/sites/iyrp.org/files/Kenya Range Management %2B Pastoralism Strategy 2021-31.pdf.

Reynolds, S. G., Suttie, J. M., & Batello, C. (2005). Grasslands of the World (Vol. 34). Food & Agriculture Org.

Richardson, A.D., 2019. Tracking seasonal rhythms of plants in diverse ecosystems with digital camera imagery. New Phytol. 222 (4), 1742–1750.

Said, M.Y., Ogutu, J.O., Kifugo, S.C., Makui, O., Reid, R.S., de Leeuw, J., 2016. Effects of extreme land fragmentation on wildlife and livestock population abundance and distribution. J. Nature Conserv. 34, 151–164. https://doi.org/10.1016/j.jnc.2016.10.005.

Seyednasrollah, B., Young, A.M., Hufkens, K., Milliman, T., Friedl, M.A., Frolking, S., Richardson, A.D., 2019. Tracking vegetation phenology across diverse biomes using Version 2.0 of the PhenoCam Dataset. Sci. Data 6 (1), 222. https://doi.org/10.1038/s41597-019-0229-9.

Skerman, P. J., Riveros, F., 1990. Tropical grasses. In FAO Plant Production and Protection Series (p. 852). FAO. https://eds.s.ebscohost.com/eds/detail/detail?vid=0&sid=9797da88-4eb0-4e3d-8869-f51246d3671f%40redis&bdata=JnNpdGU9ZWRzLWxpdmU%3D#AN=fao.629148&db=cat02127a.

Soil Survey Staff. (2014). Soil Survey Field and Laboratory Methods Manual. In United States Department of Agriculture, Natural Resources Conservation Service. doi: 10.13140/RG.2.1.3803.8889.

Sonnentag, O., Hufkens, K., Teshera-Sterne, C., Young, A.M., Friedl, M., Braswell, B.H., Milliman, T., O'Keefe, J., Richardson, A.D., 2012. Digital repeat photography for phenological research in forest ecosystems. Agric. For. Meteorol. 152, 159–177. https://doi.org/10.1016/j.agrformet.2011.09.009.

Strum, S.C., Stirling, G., Mutunga, S.K., 2015. The perfect storm: Land use change promotes Opuntia stricta's invasion of pastoral rangelands in Kenya. J. Arid Environ. 118, 37–47. https://doi.org/10.1016/j.jaridenv.2015.02.015.

Tichý, L., 2002. JUICE, software for vegetation classification. J. Veg. Sci. 13 (3), 451–453. https://doi.org/10.1111/j.1654-1103.2002.tb02069.x.

Todd, S.W., 2006. Gradients in vegetation cover, structure and species richness of Nama-Karoo shrublands in relation to distance from livestock watering points. J. Appl. Ecol. 43 (2), 293–304. https://doi.org/10.1111/j.1365-2664.2006.01154.x.

Tong, L., Liu, Y., Wang, Q., Zhang, Z., Li, J., Sun, Z., Khalifa, M., 2019. Relative effects of climate variation and human activities on grassland dynamics in Africa from 2000 to 2015. Ecol. Inf. 53, 100979 https://doi.org/10.1016/j.ecoinf.2019.100979.

Udelhoven, T., Stellmes, M., del Barrio, G., Hill, J., 2009. Assessment of rainfall and NDVI anomalies in Spain (1989–1999) using distributed lag models. Int. J. Remote Sens. 30 (8), 1961–1976.

van Vliet, A.J.H., Bron, W.A., Mulder, S., van der Slikke, W., Odé, B., 2014. Observed climate-induced changes in plant phenology in the Netherlands. Reg. Environ. Change 14 (3), 997–1008. https://doi.org/10.1007/s10113-013-0493-8.

Vrieling, A., Meroni, M., Darvishzadeh, R., Skidmore, A.K., Wang, T., Zurita-Milla, R., Oosterbeek, K., O'Connor, B., Paganini, M., 2018. Vegetation phenology from Sentinel-2 and field cameras for a Dutch barrier island. Remote Sens. Environ. 215, 517–529. https://doi.org/10.1016/j.rse.2018.03.014.

Watson, C.J., Restrepo-Coupe, N., Huete, A.R., 2019. Multi-scale phenology of temperate grasslands: improving monitoring and management with near-surface phenocams. Front. Environ. Sci. 7 (FEB), 14. https://doi.org/10.3389/fenvs.2019.00014.

Wen, Y., Liu, X., Xin, Q., Wu, J., Xu, X., Pei, F., Li, X., Du, G., Cai, Y., Lin, K., Yang, J., Wang, Y., 2019. Cumulative effects of climatic factors on terrestrial vegetation growth. J. Geophys. Res. Biogeosci. 124 (4), 789–806. https://doi.org/10.1029/2018JG004751.

Woebbecke, D.M., Meyer, G.E., Von Bargen, K., Mortensen, D.A., 1995. Color indices for weed identification under various soil, residue, and lighting conditions. Trans. ASAE 38 (1), 259–269. https://doi.org/10.13031/2013.27838.

Wu, D., Zhao, X., Liang, S., Zhou, T., Huang, K., Tang, B., Zhao, W., 2015. Time-lag effects of global vegetation responses to climate change. Glob. Change Biol. 21 (9), 3520–3531. https://doi.org/10.1111/gcb.12945.

Yan, Y., Liu, X., Wen, Y., Ou, J., 2019b. Quantitative analysis of the contributions of climatic and human factors to grassland productivity in northern China. Ecol. Ind. 103, 542–553. https://doi.org/10.1016/j.ecolind.2019.04.020.

Yan, D., Zhang, X., Nagai, S., Yu, Y., Akitsu, T., Nasahara, K.N., Ide, R., Maeda, T., 2019a. Evaluating land surface phenology from the Advanced Himawari Imager using observations from MODIS and the Phenological Eyes Network. Int. J. Appl. Earth Obs. Geoinf. 79, 71–83. https://doi.org/10.1016/j.jag.2019.02.011.

Yang, Y., Tilman, D., Furey, G., Lehman, C., 2019. Soil carbon sequestration accelerated by restoration of grassland biodiversity. Nat. Commun. 10 (1), 718. https://doi.org/10.1038/s41467-019-08636-w.

Yu, J., Wan, L., Liu, G., Ma, K., Cheng, H., Shen, Y., Liu, Y., Su, X., 2022. A meta-analysis on degraded alpine grassland mediated by climate factors: enlightenment for ecological restoration. Front. Plant Sci. 12, 3141. https://doi.org/10.3389/fpls.2021.821954.

Yu, H., Xu, J., Okuto, E., Luedeling, E., Wright, J., 2012. Seasonal response of grasslands to climate change on the Tibetan Plateau. PLoS ONE 7 (11). https://doi.org/10.1371/journal.pone.0049230.

Zarei, A., Chemura, A., Gleixner, S., Hoff, H., 2021. Evaluating the grassland NPP dynamics in response to climate change in Tanzania. Ecol. Ind. 125, 107600 https://doi.org/10.1016/j.ecolind.2021.107600.

Zhang, R., Liang, T., Guo, J., Xie, H., Feng, Q., Aimaiti, Y., 2018. Grassland dynamics in response to climate change and human activities in Xinjiang from 2000 to 2014. Sci Rep 8 (1).

Zhou, Y., Xiao, X., Wagle, P., Bajgain, R., Mahan, H., Basara, J.B., Dong, J., Qin, Y., Zhang, G., Luo, Y., Gowda, P.H., Neel, J.P.S., Starks, P.J., Steiner, J.L., 2017. Examining the short-term impacts of diverse management practices on plant phenology and carbon fluxes of Old World bluestems pasture. Agric. For. Meteorol. 237–238, 60–70. https://doi.org/10.1016/j.agrformet.2017.01.018.